ANZIAM J. 55(2014), 383–401
doi:10.1017/S1446181114000182

MOTION OF A SLIP SPHERE IN A NONCONCENTRIC FICTITIOUS SPHERICAL ENVELOPE OF MICROPOLAR FLUID

E. I. SAAD[1]

(Received 4 November, 2013; revised 12 May, 2014)

Abstract

Stokes' axisymmetrical translational motion of a slip sphere, located anywhere on the diameter of a virtual spherical fluid 'cell', is investigated. The fluid is micropolar and flows are parallel to the line connecting the two centres. An infinite-series solution is presented for the stream function, pressure field, vorticity, microrotation component, shear stress and couple stress of the flow. Basset-type slip boundary conditions on the sphere surface are used for velocity and microrotation. The Happel and Kuwabara boundary conditions are used on the fictitious surface of the cell model. Numerical results for the normalized drag force acting on the sphere are obtained with excellent convergence for various values of the volume fraction, the relative distance between the centre of the sphere and the virtual envelope, the vortex viscosity parameter and the slip coefficients of the sphere. In the special case when the spherical particle is in the concentric position with the cell surface, the numerical values of the normalized drag force agree with the available values in the literature.

2010 *Mathematics subject classification*: 76A05.

Keywords and phrases: micropolar fluid, slip condition, cell models, normalized drag force.

1. Introduction

Several non-Newtonian fluid models have been proposed to describe fluids of microstructures. Micropolar fluid, introduced by Eringen [7], is a physically relevant model that has many applications. These fluids consist of rigid, randomly oriented particles with their own spins and microrotations, suspended in a viscous medium. In micropolar fluids, rigid particles contained in a small volume element can rotate about the centre of the volume element described by the microrotation vector. In addition, individual particles can rotate independently from the rotation and movement of the fluid as a whole. Therefore, new variables which represent angular velocities of

[1]Department of Mathematics, Faculty of Science, Damanhour University, Damanhour, Egypt; e-mail: elsayedsaad74@yahoo.com.

fluid particles and new equations governing these variables should be added to the conventional model.

Micropolar theory has been applied in an increasingly significant number of cases in various scientific fields. One of them is the study of lubricating fluids in bearings in lubrication theory [19]. Ferrofluid has often been modelled as a micropolar fluid, because it consists of a stabilized colloidal suspension of Brownian magnetic particles in a nonmagnetic liquid host [25]. The micropolar fluid model is a continuum model to describe a fluid which consists of particles with internal structure [10, 13, 19]. The model equations include the asymmetric stress tensor and the couple stress tensor to describe the microrotation of constituents. Therefore, the model may be a suitable framework to describe granular flows. In fact, granular flows are flows which have microstructure and rotation of particles. Hayakawa [13] has reported that the theoretical calculations of certain boundary-value problems agree with relevant experimental results of granular flows. Cell-model techniques can be used for Newtonian or non-Newtonian fluids [5]. To the best of our knowledge, there is no previous work dealing with micropolar fluid flow in the cell model. This motivated us to pursue the present work.

The area of fluid flow relative to assemblages of particles is important in many practical applications, such as fluidization, sedimentation and flow in packed beds. Therefore, it is required to determine whether the presence of neighbouring particles and boundaries affects the movement of an individual particle. An important and successful technique that has been used in the literature [12] to predict the effect on neighbouring particles or boundaries of the motion of an individual particle is the unit-cell model. According to this model, the swarm of particles are uniformly distributed throughout the fluid phase and every particle is enclosed in the spherical cell formed by the disperse medium. Moreover, the volume of the fluid cell is chosen such that the solid volume fraction in the cell equals the solid volume fraction of the assemblage. Thus, the entire disturbance due to each particle is confined within the cell of the fluid with which it is associated. The cell model can be used to reduce the solution of the boundary-value problem for the flow around a system of particles to the problem for a single particle. Happel and Brenner [12] pointed out that although cell models of this type give an adequate approximation of the actual average flow profile close to particles in a real physical system, they cannot be expected to be valid for points close to fictitious cell boundaries.

Thus, for such points, a technique like the reflection procedure may be used. The unit-cell model has been widely used to solve boundary-value problems for solid particles in concentrated systems where the effect of the container wall may be ignored [6]. Different boundary conditions have been suggested at the fictitious surface of the cell model. Happel's model [11] assumes a uniform velocity condition and no tangential stress at the cell surface, whereas Kuwabara's model [16] assumes vanishing of vorticity instead of no tangential stress. Both models result in similar velocity fields and drag forces. Happel's model does not require an exchange of mechanical energy between the cell and the environment, while Kuwabara's model

does require such exchange. The sphere-in-cell geometry is used extensively as a simple model that can account for the hydrodynamic interactions among the spherical particles. Faltas and Saad [8] have adopted mathematical and numerical techniques to investigate the quasisteady axisymmetrical flow of an incompressible viscous fluid past an assemblage of slip eccentric spherical particle-in-cell models with Happel and Kuwabara boundary conditions. The cell technique serves as an improvement over the analysis of conventional lubrication theory. In lubrication, the fluid is usually confined in a narrow region between surfaces with a variable width. The unit-cell technique has also been used to solve boundary-value problems of the flow of a viscous fluid past a fluid sphere which has a micropolar fluid inside it as well as the related problem of a micropolar fluid past a viscous fluid drop [26]. In the literature, there are many accounts where other boundary conditions on the virtual surface have been used for the unit cell. The effect of the boundary conditions proposed by Happel, Kuwabara and Slobodov–Chepura on the velocity of a bubble ensemble in a non-Newtonian liquid was analysed in [31]. Prakash et al. [24] used the cell method to study the Stokes flow problem of an assemblage of porous particles and reviewed the known boundary proposed by Happel and Sherwood at the virtual surface. Faltas and Saad [9] have investigated the motion of a porous spherical particle placed eccentrically within a spherical cell using the Happel, Kuwabara, Kvashnin, Cunningham or Mehta–Morse boundary conditions on the cell surface.

In fluid mechanics, both no-slip and partial-slip boundary conditions were proposed in the nineteenth century [23]. Navier [22] gave the slip boundary condition, where the tangential velocity of the fluid relative to the solid at a point on its surface is proportional to the tangential stress acting at that point. For gas flows, Maxwell [20] had shown that the surface slip is related to the noncontinuous nature of the gas and the slip length is proportional to the mean-free path. For liquids, from experiments at that time, the no-slip boundary condition was accepted and since then has largely been treated as a fundamental law. However, from recent extensive studies on the surface slip in micro- and nanoscales, the physics of the fluid–solid slip is recognized to be much more complicated than that for gases. Indeed, apparent violations of the no-slip boundary condition at the fluid–solid interface in nanoscale have been reported [17, 23]. The hydrodynamic slip boundary condition has also been studied in the context of nanofluidics [4]. Basset [3] derived expressions for the force exerted by the surrounding fluid on a translating rigid sphere with a slip boundary condition at its surface (for example, a settling aerosol sphere). The hydrodynamic effects of homogeneous and nonhomogeneous slip boundary conditions for Newtonian fluids have been discussed extensively in the literature [32, 33]. Motivated by this understanding, we decided to analyse a micropolar flow problem, using the slip boundary conditions for both the velocity and the microrotation. There is no uniform consensus on the microrotation boundary conditions for micropolar fluids. An interesting review for various types of this boundary condition is given by Migun [21]. Aero et al. [1] suggested a physically acceptable dynamic boundary condition for microrotation, which states that the microrotation is proportional to the couple stress at

https://doi.org/10.1017/S1446181114000182 Published online by Cambridge University Press

the boundary. We propose a slip boundary condition for the microrotation by assuming that the tangential component of the microrotation vector of the fluid relative to the solid at a point on its surface is proportional to the corresponding tangential couple stress acting at that point. Slip boundary conditions for micropolar fluids have been used for the velocity, but not for the microrotation, by Sherief et al. and Saad [27, 29]. We think that it is physically more appropriate to use the slip boundary conditions for both the velocity and the microrotation because both conditions are applied at the same surface and the slip is mainly due to the nature of the surface and the fluid. More recently, Sherief et al. [28] used this boundary condition to study the axisymmetric rectilinear and rotary oscillations of a solid spheroidal particle in a micropolar fluid.

In the present work, the problem of the motion of a homogeneous suspension of identical spherical particles is analysed in the limit of negligible Reynolds number (Stokes flow) [15]. The effects of interaction among individual particles are taken into explicit account by employing a unit-cell model, which is known to provide good predictions for the sedimentation of monodisperse suspensions of spherical particles [12]. We assume a typical cell envelope to be spherical and the outside surface of each cell to be frictionless. Brownian motion and forces other than gravity are neglected. This study is an extension of previous work [8] for a micropolar fluid with the same geometry (see Figure 1). The slip boundary conditions for both velocity and microrotation on the spherical particle are considered. Under the Stokesian approximation, a general solution is constructed from the superposition of the basic solutions in the two spherical coordinate systems based on the particle and virtual spherical envelope. On the fictitious cell surface, Happel and Kuwabara boundary conditions are employed. A combined analytical–numerical method with the boundary collocation technique has been used to solve the field equations for micropolar fluids. The total force exerted on the solid particle settling in the fluid within a unit cell can be expressed as the sum of the gravitational forces and the buoyancy forces. The normalized drag force acting on the particle is obtained with excellent convergence for various cases of the particle relative to slip coefficients, the separation between the particle and the cell wall, and the vortex viscosity parameter. The lubrication limit is discussed as the relative distance between the centres of the particle and the cell wall approaches unity.

2. Field equations

The balance principles for mass, linear momentum and angular momentum for the steady isothermal flow of an incompressible micropolar fluid under the Stokesian assumption in the absence of body forces and body couples are given by Eringen [7]

$$\nabla \cdot \vec{q} = 0,$$
$$\nabla p + (\mu + k)\,\nabla \wedge \nabla \wedge \vec{q} - k\,\nabla \wedge \vec{v} = 0,$$
$$k\,\nabla \wedge \vec{q} - 2\,k\,\vec{v} - \gamma\,\nabla \wedge \nabla \wedge \vec{v} + (\alpha + \beta + \gamma)\,\nabla\nabla \cdot \vec{v} = 0,$$

https://doi.org/10.1017/S1446181114000182 Published online by Cambridge University Press

where $\vec{q}$, $\vec{\nu}$ and p are velocity vector, microrotation vector and pressure, respectively; μ is the dynamic viscosity coefficient; k is the vortex viscosity; α and β are the bulk spin viscosity and γ is the shear spin viscosity.

The equations for the stress tensor t_{ij} and the couple stress tensor m_{ij} are

$$t_{ij} = -p\,\delta_{ij} + \mu\,(q_{i,j} + q_{j,i}) + k\,(q_{j,i} - \epsilon_{ijm}\,\nu_m),$$
$$m_{ij} = \alpha\,\nu_{m,m}\,\delta_{ij} + \beta\,\nu_{i,j} + \gamma\,\nu_{j,i},$$

where the comma denotes partial differentiation, and δ_{ij}, ϵ_{ijm} are the Kronecker delta and the alternating tensor, respectively.

3. Statement of the problem

In the present mathematical model, we consider the quasisteady translational motion of a spherical symmetric particle of radius a in an incompressible micropolar fluid. We employ a unit-cell model, in which each spherical particle is surrounded by a nonconcentric fictitious spherical envelope of suspending fluid having an outer radius b, as shown in Figure 1. This spherical envelope is termed the cell surface. Here, (ρ, ϕ, z) and (r_2, θ_2, ϕ) denote the circular cylindrical and spherical coordinate systems, respectively, with the origin of coordinates at the centre of the cell. The centre of the particle is instantaneously located away from the cell centre at a distance d, where (r_1, θ_1, ϕ) are the spherical coordinates based on the centre of the spherical particle and the relation between r_1 and r_2 is given by $r_1^2 = r_2^2 + d^2 - 2\,r_2 d\cos\theta_2$ or $r_2^2 = r_1^2 + d^2 + 2\,r_1 d\cos\theta_1$. We assume that the particle to cell volume ratio in the unit cell is equal to the particle volume fraction φ throughout the entire suspension, that is $\varphi = (a/b)^3$. We assume that spherical particles are stationary, and steady axisymmetric flow has been established around and through them by a uniform velocity U_z directed in the positive z-direction. This is, of course, equivalent to the spherical particle at rest, while the cell surface moves in the negative z-direction with velocity U_z. The Reynolds numbers for the micropolar fluid flow are assumed to be sufficiently small so that the inertial and gyro-inertial terms in the field equations can be neglected. That is, we consider the Stokesian approximation assumption. The flow generated is axisymmetric and all the quantities are independent of ϕ due to the axial symmetry of the sphere-in-cell geometry. Therefore, we take the velocity and microrotation vectors in the directions of the unit vectors $(\vec{e}_\rho, \vec{e}_\phi, \vec{e}_z)$ of the cylindrical coordinates as

$$\vec{q} = q_\rho\,\vec{e}_\rho + q_z\,\vec{e}_z,$$
$$\vec{\nu} = \nu_\phi\,\vec{e}_\phi.$$

Since $\mathrm{div}\vec{q} = 0$, we can write the velocity components q_ρ and q_z in terms of Stokes' stream function ψ as

$$q_\rho = \frac{1}{\rho}\frac{\partial\psi}{\partial z}, \quad q_z = -\frac{1}{\rho}\frac{\partial\psi}{\partial\rho}.$$

https://doi.org/10.1017/S1446181114000182 Published online by Cambridge University Press

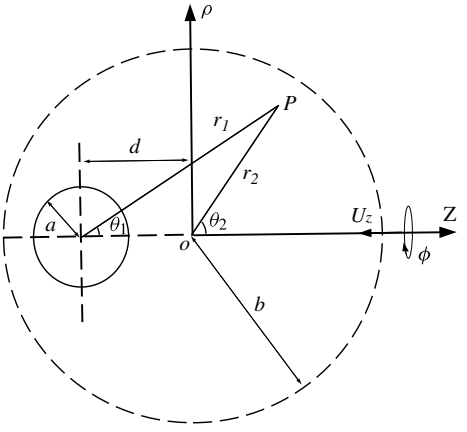

FIGURE 1. The physical situation and the description of the coordinate system for the cell model.

The problem is then governed by the following equations:

$$0 = -\frac{\partial p}{\partial \rho} - \frac{k}{\rho}\frac{\partial}{\partial z}(\rho \nu_\phi) + \frac{\mu + k}{\rho}\frac{\partial}{\partial z}(L_1 \psi), \tag{3.1}$$

$$0 = -\frac{\partial p}{\partial z} + \frac{k}{\rho}\frac{\partial}{\partial \rho}(\rho \nu_\phi) - \frac{\mu + k}{\rho}\frac{\partial}{\partial \rho}(L_1 \psi), \tag{3.2}$$

$$2\rho \nu_\phi = L_1 \psi + \frac{\gamma}{k} L_1(\rho \nu_\phi), \tag{3.3}$$

where

$$L_1 = \frac{\partial^2}{\partial \rho^2} - \frac{1}{\rho}\frac{\partial}{\partial \rho} + \frac{\partial^2}{\partial z^2}$$

is the axisymmetric Stokesian operator. After elimination of the pressure and the microrotation vector component ν_ϕ from equations (3.1)–(3.3), we get

$$L_1^2 (L_1 - \ell^2)\psi = 0, \tag{3.4}$$

with the microrotation

$$\nu_\phi = \frac{1}{2\rho}\left(L_1 \psi + \frac{2\mu + k}{k\ell^2} L_1^2 \psi\right), \tag{3.5}$$

where $\ell^2 = k(2\mu + k)/[\gamma(\mu + k)]$.

To solve equation (3.4), which is equivalent to the Stokes equations of micropolar fluid equations (3.1)–(3.3), the boundary conditions have to be specified.

At a surface of the particle $r_1 = a$, we consider the dynamical slip conditions for the velocity, and microrotations take the following forms [21, 28]:

$$q_\rho = \frac{1}{\sigma} t_{r\theta} \cos\theta_1, \tag{3.6}$$

https://doi.org/10.1017/S1446181114000182 Published online by Cambridge University Press

$$q_z = -\frac{1}{\sigma}\, t_{r\theta}\, \sin\theta_1, \tag{3.7}$$

$$v_\phi = \frac{1}{\chi}\, m_{r\phi}, \tag{3.8}$$

where $t_{r\theta}$ and $m_{r\phi}$ are the shear stress and couple stress for the flow, respectively. The constants σ and χ are termed the coefficients of sliding friction. These coefficients measure the degree of tangential slip existing between the fluid and the solid at its surface. The slip coefficients are assumed to depend only on the nature of the fluid and the solid surface. In the limiting case of $\sigma = \chi = 0$, there is a perfect slip at the surface of the sphere and the solid sphere acts like a spherical gas bubble, while the standard no-slip boundary condition for solids is obtained by letting $\sigma = \chi \to \infty$. Throughout this work, both slip coefficients are considered to be constants. The slip condition for viscous fluids has been investigated from both a physical and a rigorous mathematical point of view [18].

On the virtual surface of the cell, $r_2 = b$, we consider the following two cases:

1. *Happel model:* we assume the continuity of the radial component of velocity and vanishing of the tangential stress. Moreover, we assume that the couple stress vanishes:

$$q_\rho \tan\theta_2 + q_z = -U_z, \tag{3.9}$$

$$t_{r\theta} = 0, \tag{3.10}$$

$$m_{r\phi} = 0. \tag{3.11}$$

   The conditions (3.10) and (3.11) imply the existence of a free surface at the fictitious spherical envelope or, in other words, the slip of the liquid relative to this boundary, which can be quite acceptable from the physical point of view.
2. *Kuwabara model:* we assume again that (3.9) and (3.11) apply, but instead of the condition of vanishing tangential stress (3.10), the model uses the condition that the vorticity is equal to zero:

$$L_1^2 \psi = 0. \tag{3.12}$$

   The above condition (3.12) is physically equivalent to the absence of closed circular flows (flow circulation) at the outer cell surface.

4. Method of solution

Because of the linearity of the governing equations of motion and boundary conditions, the stream function of the fluid flow can be obtained by using the principle of superposition as [8, 12]

$$\frac{\psi}{U_z\, a^2} = \sum_{n=2}^{\infty} [\{A_n\, r_1^{-n+1} + B_n\, r_1^{-n+3} + \sqrt{r_1}\, C_n\, K_{n-\frac{1}{2}}(r_1\, \ell)\}\, \Im_n(\cos\theta_1) + \{D_n\, r_2^n + E_n\, r_2^{n+2} + \sqrt{r_2}\, F_n\, I_{n-\frac{1}{2}}(r_2\, \ell)\}\, \Im_n(\cos\theta_2)],$$

https://doi.org/10.1017/S1446181114000182 Published online by Cambridge University Press

where $\Im_n$ is the Gegenbauer polynomial of the first kind of order n and degree $-1/2$; I_m and K_m are modified Bessel functions of the first and second kinds, respectively. The coefficients A_n, B_n, C_n, D_n, E_n and F_n are unknown constants, which will be determined using the boundary conditions on the particle and the cell surfaces. Then, the microrotation component can be written as

$$\frac{a\,\nu_\phi}{U_z} = \csc\theta \sum_{n=2}^{\infty}\Big[\Big\{(3-2n)\,\frac{B_n}{r_1^n} + \frac{(\mu+k)\,\ell^2}{k\,\sqrt{r_1}}\,C_n\,K_{n-\frac{1}{2}}(r_1\,\ell)\Big\}\Im_n(\cos\theta_1) + \Big\{(2n+1)\,E_n\,r_2^{n-1} + \frac{(\mu+k)\,\ell^2}{k\,\sqrt{r_2}}\,F_n\,I_{n-\frac{1}{2}}(r_2\,\ell)\Big\}\Im_n(\cos\theta_2)\Big].$$

The corresponding pressure field is obtained by integration of the Stokes flow equations (3.1) and (3.2), so that

$$\frac{a\,p}{U_z} = -(2\mu+k)\sum_{n=2}^{\infty}\Big[\frac{(2n-3)\,B_n\,P_{n-1}(\cos\theta_1)}{n\,r_1^n} + \frac{(2n+1)\,E_n\,r_2^{n-1}\,P_{n-1}(\cos\theta_2)}{n-1}\Big],$$

where P_n is the Legendre polynomial of order n. Note that a constant of integration has been neglected without loss of generality.

The expressions for the radial and axial velocity components $(q_\rho,\ q_z)$, the microrotation component ν_ϕ, the shear stress $t_{r\theta}$ and the couple stress $m_{r\phi}$ are given by

$$q_\rho = U_z\sum_{n=2}^{\infty}[A_n\,A_{1n}(r_1,\theta_1) + B_n\,B_{1n}(r_1,\theta_1) + C_n\,C_{1n}(r_1,\theta_1) + D_n\,D_{1n}(r_2,\theta_2) + E_n\,E_{1n}(r_2,\theta_2) + F_n\,F_{1n}(r_2,\theta_2)], \tag{4.1}$$

$$q_z = U_z\sum_{n=2}^{\infty}[A_n\,A_{2n}(r_1,\theta_1) + B_n\,B_{2n}(r_1,\theta_1) + C_n\,C_{2n}(r_1,\theta_1) + D_n\,D_{2n}(r_2,\theta_2) + E_n\,E_{2n}(r_2,\theta_2) + F_n\,F_{2n}(r_2,\theta_2)], \tag{4.2}$$

$$\nu_\phi = U_z\,a^{-1}\sum_{n=2}^{\infty}[B_n\,B_{3n}(r_1,\theta_1) + C_n\,C_{3n}(r_1,\theta_1) + E_n\,E_{3n}(r_2,\theta_2) + F_n\,F_{3n}(r_2,\theta_2)], \tag{4.3}$$

$$t_{r\theta} = U_z\,a^{-1}(2\mu+k)\sum_{n=2}^{\infty}[A_n\,A_{4n}(r_1,\theta_1) + B_n\,B_{4n}(r_1,\theta_1) + C_n\,C_{4n}(r_1,\theta_1) + D_n\,D_{4n}(r_2,\theta_2) + E_n\,E_{4n}(r_2,\theta_2) + F_n\,F_{4n}(r_2,\theta_2)], \tag{4.4}$$

$$m_{r\phi} = U_z\,a^{-2}\sum_{n=2}^{\infty}[B_n\,B_{5n}(r_1,\theta_1) + C_n\,C_{5n}(r_1,\theta_1) + E_n\,E_{5n}(r_2,\theta_2) + F_n\,F_{5n}(r_2,\theta_2)], \tag{4.5}$$

$$L_1^2\psi = U_z\sum_{n=2}^{\infty}[B_n\,B_{6n}(r_1,\theta_1) + C_n\,C_{6n}(r_1,\theta_1) + E_n\,E_{6n}(r_2,\theta_2) + F_n\,F_{6n}(r_2,\theta_2)], \tag{4.6}$$

https://doi.org/10.1017/S1446181114000182 Published online by Cambridge University Press

where the functions A_{sn}, B_{sn}, C_{sn}, D_{sn}, E_{sn} and F_{sn} with $s = 1, 2, \ldots, 6$ are listed in Appendix A.

To determine the unknown constants A_n, B_n, C_n, D_n, E_n and F_n for the Happel model, we apply the boundary conditions (3.6)–(3.10), and obtain

$$0 = \sum_{n=2}^{\infty}[A_n\, a_{1n}(a,\theta_1) + B_n\, b_{1n}(a,\theta_1) + C_n\, c_{1n}(a,\theta_1) + \{D_n\, d_{1n}(r_2,\theta_2) + E_n\, e_{1n}(r_2,\theta_2) + F_n\, f_{1n}(r_2,\theta_2)\}_{r_1=a}], \tag{4.7}$$

$$0 = \sum_{n=2}^{\infty}[A_n\, a_{2n}(a,\theta_1) + B_n\, b_{2n}(a,\theta_1) + C_n\, c_{2n}(a,\theta_1) + \{D_n\, d_{2n}(r_2,\theta_2) + E_n\, e_{2n}(r_2,\theta_2) + F_n\, f_{2n}(r_2,\theta_2)\}_{r_1=a}], \tag{4.8}$$

$$0 = \sum_{n=2}^{\infty}[B_n\, b_{3n}(a,\theta_1) + C_n\, c_{3n}(a,\theta_1) + \{E_n\, e_{3n}(r_2,\theta_2) + F_n\, f_{3n}(r_2,\theta_2)\}_{r_1=a}], \tag{4.9}$$

$$-1 = \sum_{n=2}^{\infty}[\{A_n\, a_{4n}(r_1,\theta_1) + B_n\, b_{4n}(r_1,\theta_1) + C_n\, c_{4n}(r_1,\theta_1)\}_{r_2=b} + D_n\, d_{4n}(b,\theta_2) + E_n\, e_{4n}(b,\theta_2) + F_n\, f_{4n}(b,\theta_2)], \tag{4.10}$$

$$0 = \sum_{n=2}^{\infty}[\{A_n\, A_{4n}(r_1,\theta_1) + B_n\, B_{4n}(r_1,\theta_1) + C_n\, C_{4n}(r_1,\theta_1)\}_{r_2=b} + D_n\, D_{4n}(b,\theta_2) + E_n\, E_{4n}(b,\theta_2) + F_n\, F_{4n}(b,\theta_2)], \tag{4.11}$$

$$0 = \sum_{n=2}^{\infty}[\{B_n\, B_{5n}(r_1,\theta_1) + C_n\, C_{5n}(r_1,\theta_1)\}_{r_2=b} + E_n\, E_{5n}(b,\theta_2) + F_n\, F_{5n}(b,\theta_2)] \tag{4.12}$$

and, for the Kuwabara model, equation (4.11) is replaced by

$$0 = \sum_{n=2}^{\infty}\{[B_n\, B_{6n}(r_1,\theta_1) + C_n\, C_{6n}(r_1,\theta_1)]_{r_2=b} + E_n\, E_{6n}(b,\theta_2) + F_n\, F_{6n}(b,\theta_2)\}, \tag{4.13}$$

where the expressions for a_{kn}, b_{kn}, c_{kn}, d_{kn}, e_{kn} and f_{kn}, with $k = 1, 2, 3, 4$, are also given in Appendix A. To determine the fluid velocity and pressure, the boundary conditions (4.7)–(4.12) (or (4.7)–(4.10), (4.12) and (4.13)) should be satisfied exactly along the particle and cell surfaces. This would result in infinite linear algebraic equations for infinitely many unknown coefficients, which are impossible to solve. The multipole collocation technique [14] is used to truncate the infinite series in equations (4.1)–(4.6) after N terms, and to satisfy the boundary conditions mentioned above at N discrete points on each longitudinal arc of the particle and cell surfaces. This leads to a system of $6N$ simultaneous linear algebraic equations. This matrix equation can be solved by any matrix-reduction technique to yield the $6N$ unknown constants A_n, B_n, C_n, D_n, E_n and F_n appearing in the truncated form of equations (4.1)–(4.6).

https://doi.org/10.1017/S1446181114000182 Published online by Cambridge University Press

The fluid flow field is completely obtained once these constants are solved for a sufficiently large value of N. In all subsequent expressions in this paper, r and r_j are nondimensional with respect to the porous sphere of radius a.

The hydrodynamic drag force F_z exerted on the particle surface $r_1 = 1$ in a cell by the external fluid can be evaluated as

$$\begin{aligned} F_z &= 2\pi a^2 \int_0^\pi r^2 \left(t_{rr}\cos\theta - t_{r\theta}\sin\theta\right)|_{r=1} \ \sin\theta\, d\theta \\ &= 2\pi a^2(2\mu + k)\int_0^\pi r^2 \left[\left\{\frac{-p}{2\mu + k} + \frac{\partial}{\partial r}\left(\frac{1}{r^2}\frac{\partial \psi}{\partial \cos\theta}\right)\right\}\cos\theta - \frac{\partial}{\partial r}\left(\frac{1}{r}\frac{\partial \psi}{\partial r}\right)\right. \\ &\quad \left. + \frac{1}{2r\,\ell^2} L_{-1}(L_{-1} + \ell^2)\psi\right]\Bigg|_{r=1} \sin\theta\, d\theta = 2\pi a\, U_z(2\mu + k)B_2. \end{aligned} \tag{4.14}$$

The above expression shows that only the lowest-order coefficient B_2 contributes to the hydrodynamic force acting on the particle. In fact, the coefficient B_2 is the most accurate (fastest-convergent) result obtainable from the boundary collocation method [8, 14].

For the slow translation of a slip sphere situated at the cell centre, the exact solution of the drag force on the spherical particle with the same type of the boundary conditions at the fictitious surface is given in Appendix B. The drag force on a slip spherical particle in the case of uniform streaming in an unbounded micropolar fluid is also derived in Appendix B. The normalized drag force W_c is defined as the ratio of the actual drag experienced by the sphere in the cell surface to the drag on a sphere in an infinite expansion of fluid. With the aid of equations (4.14) and (B.9), this becomes

$$W_c = \frac{(3 + 2\lambda)(\mu + k)(\ell^2 + \delta(1 + \ell)) - k\,\delta(1 + \lambda)}{3(\mu + k)(1 + \lambda)(\ell^2 + \delta(1 + \ell))} B_2,$$

where $\delta = \gamma^{-1}(\chi a + 2\gamma + \beta)$ and $\lambda = \sigma a/(2\mu + k)$. Note that $W_c = 1$ as $a/(b - d) = 0$ for any specified values of λ and δ.

The presence of the virtual surface of the unit cell always enhances the hydrodynamic drag on the particle, since the radial fluid flow vanishes there. For the model under consideration, the drag force per particle multiplied by the number of particles per unit volume is balanced by the pressure drop per unit length of the particle bed due to passage of fluid through it as

$$\frac{(a/b)^3 F_z}{4\pi a^3/3} = -\frac{\Delta P}{L}. \tag{4.15}$$

Hence, from equations (4.14) and (4.15), we get the superficial fluid velocity through the bed of porous spherical particles as

$$U_z = \left(-\frac{a^2}{3\varphi B_2}\right)\frac{\Delta P}{(\mu + k/2)L}.$$

The expression in parentheses is the permeability coefficient in Darcy's law. This law was obtained empirically by Darcy in experiments with water flow through sand filters.

https://doi.org/10.1017/S1446181114000182 Published online by Cambridge University Press

If we use $U_z^{(0)}$ and $\Delta P^{(0)}$ to represent U_z and ΔP, respectively, as $\varphi \to 0$ (for a dilute medium), the ratio $U_z/U_z^{(0)}$ with $\Delta P = \Delta P^{(0)}$ (equals the ratio $\Delta P^{(0)}/\Delta P$ with $U_z = U_z^{(0)}$) is also equal to the inverse normalized drag force (that is W_c^{-1}).

4.1. Results When specifying the points along the semi-circular generating arcs of the solid sphere and cell surfaces where the boundary conditions are exactly satisfied, the first two points that should be chosen are $\theta_{1,2} = 0$ and π, since these points control the extreme gaps between the particle and the cell surfaces. In addition, the points $\theta_{1,2} = \pi/2$ are also important. However, an examination of the systems of linear algebraic equations for the unknown constants A_n, B_n, C_n and D_n shows that the coefficient matrix becomes singular if these points are used. In order to avoid this singular matrix and achieve good accuracy, we adopt the method recommended in the literature [8, 14] to choose the collocation points as follows. On the half unit circle $0 \le \theta_{1,2} \le \pi$ in any meridional plane, $\theta_{1,2} = \varepsilon$, $\pi/2 - \varepsilon$, $\pi/2 + \varepsilon$ and $\pi - \varepsilon$ are taken as four basic multipoles, where ε is specified by a small value, so that the singularities at $\theta_{1,2} = 0$, $\pi/2$, and π can be avoided. The other points are selected as mirror-image pairs of $\theta_{1,2} = \pi/2$, which are evenly distributed on the two quarter circles, excluding those singularity points. A Gaussian elimination method is used to solve the linear equations to determine the coefficients. The normalized drag force is then calculated.

The collocation solutions of the normalized drag for both cases of Happel and Kuwabara models are presented in Figures 2–5, when the parameters are given by $\gamma/\mu a^2 = 0.3$, $\beta/\mu a^2 = 0.2$ for various values of the following parameters:

(1) the solid volume fraction, φ ($0 < \varphi \le 0.74$);
(2) the vortex viscosity parameter k/μ;
(3) the relative distance between the centres of the particle and cell δ ($= d/(b - a)$);
(4) the slip coefficients of the particle $\sigma a/\mu$ and $\chi/\mu a$.

The accuracy and convergence behaviour of the boundary-collocation and truncation technique depends mainly upon the ratios δ and φ. For the difficult case of $\delta = 0.99$, the number of collocation points $N = 150$ is sufficiently large to achieve this convergence. The results are presented up to $\varphi = 0.74$, which corresponds to the maximum possible volume fraction for an assemblage of identical spherical particles [30]. It is also clear that at volume fractions approaching this value, accumulation due to contacts between particles may occur, and the present model will not give satisfactory results. However, a solid volume fraction close to unity is geometrically possible.

The results in Figure 2 show that the normalized drag, W_c, force exerted on the spherical particle increases monotonically with an increase in φ or δ, when the other parameters are fixed. Also, this drag, in general, increases as $\sigma a/\mu$ increases while keeping the other parameters unchanged. Figure 3 indicates that W_c decreases monotonically with an increase in k/μ for any specified values of φ, but at fixed values of the other variables. For the Newtonian fluid situation, $k/\mu = 0$, the normalized drag force is at a maximum. Interestingly, for constant values of φ, $\sigma a/\mu$, $\chi/\mu a$, k/μ and δ, the Kuwabara model predicts larger values of the normalized drag force on a slip

https://doi.org/10.1017/S1446181114000182 Published online by Cambridge University Press

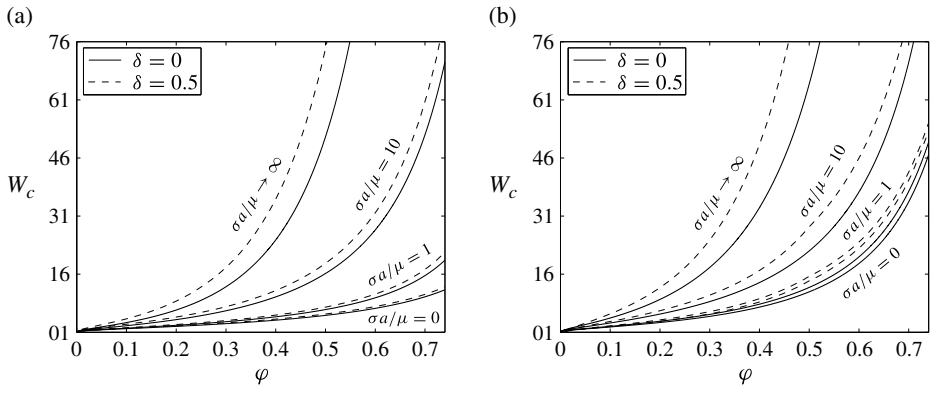

FIGURE 2. Normalized drag force distribution for different values of $\sigma a/\mu$ and δ with $\chi/\mu\, a = \sigma a/\mu$ and $k/\mu = 2$. (a) Happel cell model calculations; (b) Kuwabara cell model calculations.

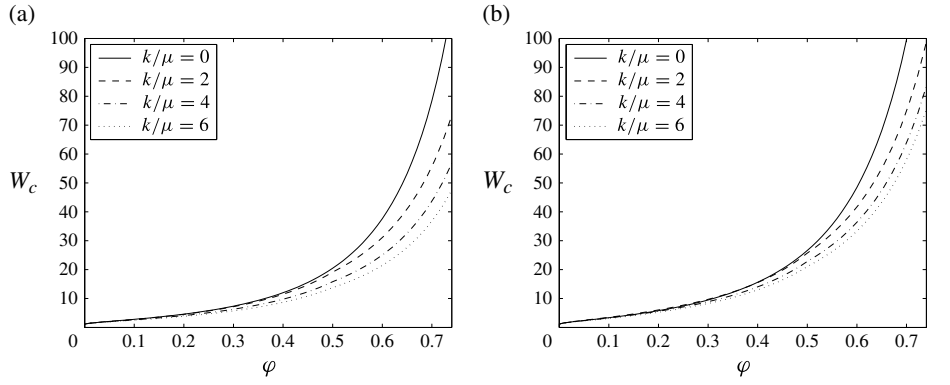

FIGURE 3. Normalized drag force distribution for different values of k/μ with $\sigma a/\mu = \chi/\mu\, a = 10$ and $\delta = 0.25$. (a) Happel cell model calculations; (b) Kuwabara cell model calculations.

spherical particle than the Happel model does. This occurs because the zero-vorticity model yields a larger energy dissipation in the cell than that due to particle drag alone, owing to the additional work done by the stresses at the outer boundary [12]. The predictions of the two models, in general, result in the same behaviour qualitatively and are in numerical agreement with each other within 5–23% (see Figure 4). Also, it can be observed that the normalized drag has its minimal value when the particle is in the concentric position inside the virtual envelope ($\delta = 0$). In the lubrication limit, the micropolar fluid is confined in a narrow region and occurs as $\delta \approx 1$, where in this case the drag force increases indefinitely. Figure 5 shows that the drag force is finite in both the perfect slip and no-slip limits. It indicates also that for the entire range of the slip parameter, W_c increases with the increase of volume fraction parameter for both models.

https://doi.org/10.1017/S1446181114000182 Published online by Cambridge University Press

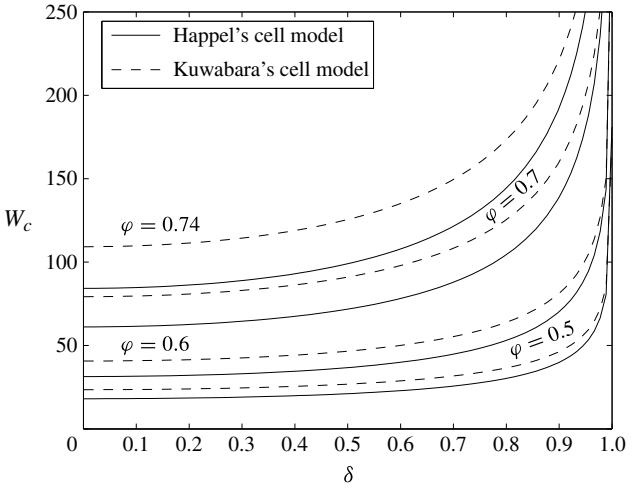

FIGURE 4. Normalized drag force distribution for different values of φ with $\sigma a/\mu = \chi/\mu a = 10$ and $k/\mu = 1$.

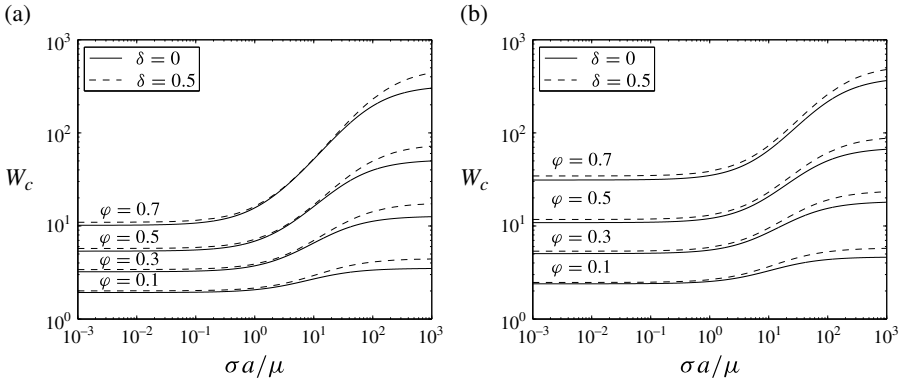

FIGURE 5. Normalized drag force distribution for different values of φ and δ with $\chi/\mu a = 10$ and $k/\mu = 3$. (a) Happel cell model calculations; (b) Kuwabara cell model calculations.

5. Conclusion

A combined analytical–numerical solution for the slow motion of a micropolar fluid past a spherical particle, via the particle-in-cell model, along the line connecting their centres is presented using the Happel and Kuwabara cell models. The field equations for micropolar fluids are solved and the hydrodynamic drag force acting on the particle has been calculated for a range of parameters. As expected, the normalized drag force is a monotonically increasing function of the solid volume fraction for the two models, but it decreases as the vortex viscosity parameter increases. For a constant value of volume fraction, the normalized drag force is minimal when the particle is situated at the cell centre, and increases monotonically with the relative distance between the

https://doi.org/10.1017/S1446181114000182 Published online by Cambridge University Press

centres of the particle and the cell wall. Clearly, the normalized drag force acting on the particle increases with its increasing slip coefficient while keeping the other parameters unchanged. In general, the vortex viscosity parameter depends on the shape and concentration of the microelements. For a given shape of the microelements, k/μ directly gives a measure of concentration of the microelements [2]. It is observed that the drag in a micropolar fluid is smaller than that in a Newtonian fluid. However, at this stage, no experimental data is available in the literature that indicates how particles interact in an assemblage. Experiments are needed to prove the validity of the theoretical results obtained in this study for the cell model at various values of the particle's relative slip coefficients, the vortex viscosity parameter and the solid volume fraction.

Appendix A

The functions appearing in equations (4.1)–(4.6) are defined as

$$
\begin{aligned}
A_{1n}(r,\theta) &= -r^{-n-1}\,(n+1)\,\Im_{n+1}(\cos\theta)\,\csc\theta,\\
B_{1n}(r,\theta) &= -r^{1-n}\,[(n+1)\,\Im_{n+1}(\cos\theta)\,\csc\theta - 2\Im_n(\cos\theta)\,\cot\theta],\\
C_{1n}(r,\theta) &= -r^{-3/2}\,[(n+1)\,K_{n-\frac{1}{2}}(r\ell)\,\Im_{n+1}(\cos\theta)\,\csc\theta + r\ell\,K_{n-\frac{3}{2}}(r\ell)\,\Im_n(\cos\theta)\,\cot\theta],\\
D_{1n}(r,\theta) &= -r^{n-2}\,((n+1)\,\Im_{n+1}(\cos\theta)\,\csc\theta - (2n-1)\,\Im_n(\cos\theta)\,\cot\theta),\\
E_{1n}(r,\theta) &= -r^{n}\,[(n+1)\,\Im_{n+1}(\cos\theta)\,\csc\theta - (2n+1)\,\Im_n(\cos\theta)\,\cot\theta],\\
F_{1n}(r,\theta) &= -r^{-3/2}\,[(n+1)\,I_{n-\frac{1}{2}}(r\ell)\,\Im_{n+1}(\cos\theta)\,\csc\theta - r\ell\,I_{n-\frac{3}{2}}(r\ell)\,\Im_n(\cos\theta)\,\cot\theta],\\
A_{2n}(r,\theta) &= -r^{-n-1}\,P_n(\cos\theta),\\
B_{2n}(r,\theta) &= -r^{1-n}\,[2\,\Im_n(\cos\theta) + P_n(\cos\theta)],\\
C_{2n}(r,\theta) &= r^{-3/2}\,[r\ell\,K_{n-\frac{3}{2}}(r\ell)\,\Im_n(\cos\theta) - K_{n-\frac{1}{2}}(r\ell)\,P_n(\cos\theta)],\\
D_{2n}(r,\theta) &= r^{n-2}\,((1-2n)\,\Im_n(\cos\theta) - P_n(\cos\theta)),\\
E_{2n}(r,\theta) &= -r^{n}\,[(1+2n)\,\Im_n(\cos\theta) + P_n(\cos\theta)],\\
F_{2n}(r,\theta) &= -r^{-3/2}\,(r\ell\,I_{n-\frac{3}{2}}(r\ell)\,\Im_n(\cos\theta) + I_{n-\frac{1}{2}}(r\ell)\,P_n(\cos\theta)),\\
B_{3n}(r,\theta) &= r^{-n}\,(3-2n)\,\Im_n(\cos\theta)\,\csc\theta,\\
C_{3n}(r,\theta) &= r^{-1/2}\,k^{-1}\,\ell^2\,(\mu+k)\,K_{n-\frac{1}{2}}(r\ell)\,\Im_n(\cos\theta)\,\csc\theta,\\
E_{3n}(r,\theta) &= (1+2n)\,r^{n-1}\,\Im_n(\cos\theta)\,\csc\theta,\\
F_{3n}(r,\theta) &= r^{-1/2}\,k^{-1}\,\ell^2\,(\mu+k)\,I_{n-\frac{1}{2}}(r\ell)\,\Im_n(\cos\theta)\,\csc\theta,\\
A_{4n}(r,\theta) &= (n^2-1)\,r^{-n-2}\,\Im_n(\cos\theta)\,\csc\theta,\\
B_{4n}(r,\theta) &= n\,(n-2)\,r^{-n}\,\Im_n(\cos\theta)\,\csc\theta,\\
C_{4n}(r,\theta) &= r^{-5/2}\,[n\,(n-2)\,K_{n-\frac{1}{2}}(r\ell) + r\ell\,K_{n+\frac{1}{2}}(r\ell)]\,\Im_n(\cos\theta)\,\csc\theta,\\
D_{4n}(r,\theta) &= n\,(n-2)\,r^{n-3}\,\Im_n(\cos\theta)\,\csc\theta,
\end{aligned}
$$

https://doi.org/10.1017/S1446181114000182 Published online by Cambridge University Press

$$
\begin{aligned}
E_{4n}(r,\theta) &= (n^2-1)\, r^{n-1}\, \Im_n(\cos\theta)\, \csc\theta,\\
F_{4n}(r,\theta) &= r^{-5/2}\, (n\,(n-2)\, I_{n-\frac{1}{2}}(r\ell) - r\ell\, I_{n+\frac{1}{2}}(r\ell))\, \Im_n(\cos\theta)\, \csc\theta,\\
B_{5n}(r,\theta) &= r^{-n-1}\, (2n-3)\, (\gamma\, n+\beta)\, \Im_n(\cos\theta)\, \csc\theta,\\
C_{5n}(r,\theta) &= r^{-3/2}\, (2\mu+k)\, [(n-1-\beta/\gamma)\, K_{n-\frac{1}{2}}(r\ell) - r\,\ell\, K_{n+\frac{1}{2}}(r\ell)]\, \Im_n(\cos\theta)\, \csc\theta,\\
E_{5n}(r,\theta) &= r^{n-2}\, (2n+1)\, (\gamma\, n-\beta-\gamma)\, \Im_n(\cos\theta)\, \csc\theta,\\
F_{5n}(r,\theta) &= r^{-3/2}\, (2\mu+k)\, [(n-1-\beta/\gamma)\, I_{n-\frac{1}{2}}(r\ell) + r\,\ell\, I_{n+\frac{1}{2}}(r\ell)]\, \Im_n(\cos\theta)\, \csc\theta,\\
B_{6n}(r,\theta) &= 2r^{-n+1}\, (3-2n)\, \Im_n(\cos\theta),\\
C_{6n}(r,\theta) &= r^{1/2}\, \ell^2\, K_{n-\frac{1}{2}}(r\ell)\, \Im_n(\cos\theta),\\
E_{6n}(r,\theta) &= 2(1+2n)\, r^n\, \Im_n(\cos\theta),\\
F_{6n}(r,\theta) &= r^{1/2}\, \ell^2\, I_{n-\frac{1}{2}}(r\ell)\, \Im_n(\cos\theta).
\end{aligned}
$$

Also, the functions appearing in equations (4.7)–(4.10) are defined as

$$
\begin{aligned}
a_{1n}(r,\theta) &= A_{1n}(r,\theta) - \sigma^{-1}\, A_{4n}(r,\theta)\, \cos\theta_1,\\
b_{1n}(r,\theta) &= B_{1n}(r,\theta) - \sigma^{-1}\, B_{4n}(r,\theta)\, \cos\theta_1,\\
c_{1n}(r,\theta) &= C_{1n}(r,\theta) - \sigma^{-1}\, C_{4n}(r,\theta)\, \cos\theta_1,\\
d_{1n}(r,\theta) &= D_{1n}(r,\theta) - \sigma^{-1}\, D_{4n}(r,\theta)\, \cos\theta_1,\\
e_{1n}(r,\theta) &= E_{1n}(r,\theta) - \sigma^{-1}\, E_{4n}(r,\theta)\, \cos\theta_1,\\
f_{1n}(r,\theta) &= F_{1n}(r,\theta) - \sigma^{-1}\, F_{4n}(r,\theta)\, \cos\theta_1,\\
a_{2n}(r,\theta) &= A_{2n}(r,\theta) + \sigma^{-1}\, A_{4n}(r,\theta)\, \sin\theta_1,\\
b_{2n}(r,\theta) &= B_{2n}(r,\theta) + \sigma^{-1}\, B_{4n}(r,\theta)\, \sin\theta_1,\\
c_{2n}(r,\theta) &= C_{2n}(r,\theta) + \sigma^{-1}\, C_{4n}(r,\theta)\, \sin\theta_1,\\
d_{2n}(r,\theta) &= D_{2n}(r,\theta) + \sigma^{-1}\, D_{4n}(r,\theta)\, \sin\theta_1,\\
e_{2n}(r,\theta) &= E_{2n}(r,\theta) + \sigma^{-1}\, E_{4n}(r,\theta)\, \sin\theta_1,\\
f_{2n}(r,\theta) &= F_{2n}(r,\theta) + \sigma^{-1}\, F_{4n}(r,\theta)\, \sin\theta_1,\\
b_{3n}(r,\theta) &= B_{3n}(r,\theta) - \chi^{-1}\, B_{5n}(r,\theta),\\
c_{3n}(r,\theta) &= C_{3n}(r,\theta) - \chi^{-1}\, C_{5n}(r,\theta),\\
e_{3n}(r,\theta) &= E_{3n}(r,\theta) - \chi^{-1}\, E_{5n}(r,\theta),\\
f_{3n}(r,\theta) &= F_{3n}(r,\theta) - \chi^{-1}\, F_{5n}(r,\theta),\\
a_{4n}(r,\theta) &= A_{1n}(r,\theta)\, \tan\theta_2 + A_{2n}(r,\theta),\\
b_{4n}(r,\theta) &= B_{1n}(r,\theta)\, \tan\theta_2 + B_{2n}(r,\theta),\\
c_{4n}(r,\theta) &= C_{1n}(r,\theta)\, \tan\theta_2 + C_{2n}(r,\theta),\\
d_{4n}(r,\theta) &= D_{1n}(r,\theta)\, \tan\theta_2 + D_{2n}(r,\theta),\\
e_{4n}(r,\theta) &= E_{1n}(r,\theta)\, \tan\theta_2 + E_{2n}(r,\theta),\\
f_{4n}(r,\theta) &= F_{1n}(r,\theta)\, \tan\theta_2 + F_{2n}(r,\theta).
\end{aligned}
$$

https://doi.org/10.1017/S1446181114000182 Published online by Cambridge University Press

Appendix B. Translation of a slip sphere in a concentric virtual spherical cell

For the purpose of comparison, we consider the quasisteady translational motion of a slip spherical particle of radius a in a concentric fictitious spherical cell of radius b filled with an incompressible micropolar fluid. Under the assumption of Stokesian flow, the stream function ψ and the microrotation component ν_ϕ satisfy equations (3.4) and (3.5), respectively.

The boundary conditions used here are as follows:

- At the particle surface ($r = 1$):
  The normal component of the fluid velocity vanishes:

$$\psi = 0. \tag{B.1}$$

Slip conditions at its surface are

$$\lambda \frac{\partial \psi}{\partial r} = 2r \frac{\partial}{\partial r}\left(\frac{1}{r}\frac{\partial \psi}{\partial r}\right) - L_{-1}\psi, \tag{B.2}$$

$$\chi\, a\, \nu_\phi = \gamma \frac{\partial \nu_\phi}{\partial r} - \beta \frac{\nu_\phi}{r}. \tag{B.3}$$

- At the virtual surface of cell model ($r = b/a$ or $r = \eta^{-1}$):
  Continuity of normal velocity given by

$$\frac{\partial \psi}{\partial \theta} = U_z\, a^2\, r^2\, \sin\theta \cos\theta. \tag{B.4}$$

According to Happel [11], the tangential stress vanishes, and the couple stress is equal to zero at the virtual boundary of the cell:

$$2r \frac{\partial}{\partial r}\left(\frac{1}{r}\frac{\partial \psi}{\partial r}\right) - L_{-1}\psi = 0, \tag{B.5}$$

$$\gamma \frac{\partial \nu_\phi}{\partial r} - \beta \frac{\nu_\phi}{r} = 0. \tag{B.6}$$

The solution to equations (3.4) and (3.5) suitable for satisfying the boundary conditions on the spherical and virtual cell surfaces for the stream function and the microrotation component in the spherical coordinates is given by Happel and Brenner [12] and Saad [27]

$$\frac{\psi}{U_z\, a^2} = \left[A\, r^{-1} + B\, r + D\, r^2 + E\, r^4 + \sqrt{r}\, C\, K_{\frac{3}{2}}(r\ell) + \sqrt{r}\, F\, I_{\frac{3}{2}}(r\ell)\right] \Im_2(\cos\theta),$$

$$\frac{a\, \nu_\phi}{U_z} = \left[-\frac{B}{r^2} + 5E\, r + \frac{(\mu + k)\, \ell^2}{k\, \sqrt{r}}\, C\, K_{\frac{3}{2}}(r\ell) + \frac{(\mu + k)\, \ell^2}{k\, \sqrt{r}}\, F\, I_{\frac{3}{2}}(r\ell)\right] \Im_2(\cos\theta)\, \csc\theta, \tag{B.7}$$

where A, B, C, D, E and F are arbitrary constants to be determined from the above boundary conditions (B.1)–(B.6).

https://doi.org/10.1017/S1446181114000182 Published online by Cambridge University Press

Using formula (4.14), the drag force is found to be

$$F_z = 2\pi a U_z (2\mu + k) B. \tag{B.8}$$

When $b \to \infty$ (or $\eta = 0$), the drag on a solid sphere with slip in the case of uniform streaming in an unbounded micropolar fluid is

$$F_{z\infty} = \frac{-6\pi a U_z (2\mu + k)(\mu + k)(1 + \lambda)[\ell^2 + \delta(1 + \ell)]}{(3 + 2\lambda)(\mu + k)[\ell^2 + \delta(1 + \ell)] - k\delta(1 + \lambda)}. \tag{B.9}$$

As $\chi \to \infty$, the drag on the sphere is found to be

$$F_{z\infty} = -\frac{6\pi a U_z (2\mu + k)(\mu + k)(1 + \ell)(1 + \lambda)}{(\mu + k)(2\lambda + 3)(1 + \ell) - k(1 + \lambda)},$$

a result previously obtained by Saad [27].

For perfect slip ($\sigma = \chi \to 0$), the drag reduces to

$$F_{z\infty} = -\frac{6\pi a U_z (2\mu + k)(\mu + k)[\gamma \ell^2 + (2\gamma + \beta)(1 + \ell)]}{3(\mu + k)[\gamma \ell^2 + (2\gamma + \beta)(1 + \ell)] - k(2\gamma + \beta)}$$

for the slow translation of a slip solid sphere located at the centre of a fictitious spherical envelope in an axisymmetric viscous fluid based on Happel's model. The exact expression of its normalized drag force is obtained explicitly as

$$\begin{aligned} W_c = &-\frac{\sigma a + 3\mu}{\sigma a + 2\mu}\left[\frac{2}{3}(\sigma a - 3\mu)\varphi^{5/3} + \sigma a + 2\mu\right] \\ &\times\left[(\sigma a - 3\mu)\varphi^2 - \frac{3}{2}(\sigma a - 2\mu)\varphi^{5/3} + \frac{3}{2}(\sigma a + 2\mu)\varphi^{1/3} - \sigma a - 3\mu\right]^{-1}. \end{aligned} \tag{B.10}$$

This is in agreement with the result obtained by Faltas and Saad [8].

A different approach, which was developed by Kuwabara [16], is based on the assumption that the curl of the velocity at the fictitious surface of the cell is equal to zero. In this case, equation (B.5) is replaced by vanishing of vorticity:

$$L_1^2 \psi = 0. \tag{B.11}$$

With this change, the stream functions and the drag force can still be expressed in the forms of equations (B.7) and (B.8), but the values of unknown constants should be determined by boundary conditions (B.2)–(B.4), (B.6) and (B.11).

Therefore, for the viscous fluid of the Kuwabara model, the normalized drag force on a slip spherical particle is given by

$$W_c = (\sigma a + 3\mu)[\sigma a + 3\mu - \varphi^{1/3}\{\tfrac{1}{5}(\sigma a - 3\mu)\varphi^{5/3} - \sigma a \varphi^{2/3} + \tfrac{9}{5}(\sigma a + 2\mu)\}]^{-1}.$$

https://doi.org/10.1017/S1446181114000182 Published online by Cambridge University Press

References

[1] E. L. Aero, A. N. Bulygin and E. V. Kuvshinskii, "Asymmetric hydromechanics", *J. Appl. Math. Mech.* **29** (1965) 333–346; doi:10.1016/0021-8928(65)90035-3.

[2] Z. Alloui, H. Beji and P. Vasseur, "Double-diffusive and Soret-induced convection of a micropolar fluid in a vertical channel", *Comput. Math. Appl.* **62** (2011) 725–736; doi:10.1016/j.camwa.2011.05.053.

[3] B. B. Basset, *A treatise on hydrodynamics* 2 (Dover, New York, 1961).

[4] L. Bocquet and E. Charlaix, "Nanofluidics, from bulk to interfaces", *Chem. Soc. Rev.* **39** (2010) 1073–1095; doi:10.1039/B909366B.

[5] R. P. Chhabra, J. Comiti and I. Machac, "Flow of non-Newtonian fluids in fixed and fluidised beds", *Chem. Engrg. Sci.* **56** (2001) 1–27; doi:10.1016/S0009-2509(00)00207-4.

[6] G. Dassios, M. Hajinicolaou, F. A. Coutelieris and A. Payatakes, "Stokes flow in spheroidal particle-in-cell models with Happel and Kuwabara boundary conditions", *Internat. J. Engrg. Sci.* **33** (1995) 1465–1490; doi:10.1007/s00707-008-0048-0.

[7] A. C. Eringen, *Microcontinuum field theories II: fluent media* (Springer, New York, 2001).

[8] M. S. Faltas and E. I. Saad, "Stokes flow past an assemblage of slip eccentric spherical particle-in-cell models", *Math. Methods Appl. Sci.* **34** (2011) 1594–1605; doi:10.1002/mma.1465.

[9] M. S. Faltas and E. I. Saad, "Slow motion of porous eccentric spherical particle-in-cell models", *Transp. Porous Media* **95** (2012) 133–150; doi:10.1007/s11242-012-0036-7.

[10] B. Gayen and M. Alam, "Algebraic and exponential instabilities in a sheared micropolar granular fluid", *J. Fluid Mech.* **567** (2006) 195–233; doi:10.1017/S002211200600214X.

[11] J. Happel, "Viscous flow in multiparticle systems: slow motion of fluids relative to beds of spherical particles", *AIChE J.* **4** (1958) 197–201.

[12] J. Happel and H. Brenner, *Low Reynolds number hydrodynamics* (Martinus Nijoff, The Hague, Netherlands, 1983).

[13] H. Hayakawa, "Slow viscous flows in micropolar fluids", *Phys. Rev. E* **61** (2000) 5477–5492; doi:10.1103/PhysRevE.61.5477.

[14] H. J. Keh and T. C. Lee, "Axisymmetric creeping motion of a slip spherical particle in a nonconcentric spherical cavity", *Theoret. Comput. Fluid Dyn.* **24** (2010) 497–510; doi:10.1016/j.ijengsci.2013.03.010.

[15] B. J. Kirby, *Micro- and nanoscale fluid mechanics: transport in microfluidic devices* (Cambridge University Press, Cambridge, 2010).

[16] S. Kuwabara, "The forces experienced by randomly distributed parallel circular cylinders or spheres in a viscous flow at small Reynolds numbers", *J. Phys. Soc. Japan* **14** (1959) 527–532.

[17] E. Lauga, M. P. Brenner and H. A. Stone, *Handbook of experimental fluid dynamics* (Springer, New York, 2007); doi:10.1007/9783540302995.

[18] T. Lee, E. Charrault and C. Neto, "Interfacial slip on rough, patterned and soft surfaces: a review of experiments and simulations", *Adv. Colloid Interface Sci.* **210** (2014) 21–38; doi:10.1016/j.cis.2014.02.015.

[19] G. Łukaszewicz, *Micropolar fluids: theory and applications* (Birkhäuser, Basel, 1999).

[20] J. C. Maxwell, "On stresses in rarified gases arising from inequalities of temperature", *Philos. Trans. R. Soc. Lond.* **170** (1879) 231–256.

[21] N. P. Migun, "On hydrodynamic boundary conditions for microstructural fluids", *Rheol. Acta* **23** (1984) 575–581; doi:10.1007/BF01438797.

[22] C. L. M. H. Navier, "Mémoire sur les lois du mouvement des fluids", *Mem. Acad. R. Sci. Inst. France* **6** (1823) 389–416.

[23] C. Neto, D. R. Evans, E. Bonaccurso, H. J. Butt and V. S. J. Craig, "Boundary slip in Newtonian liquids: a review of experimental studies", *Rep. Progr. Phys.* **68** (2005) 2859–2897; doi:10.1088/00344885/68/12/R05.

[24] J. Prakash, G. P. Raja Sekhar and M. Kohr, "Stokes flow of an assemblage of porous particles: stress jump condition", *Z. Angew. Math. Phys.* **62** (2011) 1027–1046; doi:10.1007/s00033-011-0123-6.

[25] R. E. Rosensweig and R. J. Johnston, "Aspects of magnetic fluid flow with nonequilibrium magnetization", in: *Continuum mechanics and its applications* (eds G. A. C. Graham and S. K. Malik), (Hemisphere, New York, 1989), 707–729.
[26] E. I. Saad, "Cell models for micropolar flow past a viscous fluid sphere", *Meccanica* **47** (2012) 2055–2068; doi:10.1007/s11012-012-9575-9.
[27] E. I. Saad, "Motion of a spheroidal particle in a micropolar fluid contained in spherical envelope", *Canad. J. Phys.* **86** (2008) 1039–1056; doi:10.1139/P08045.
[28] H. H. Sherief, M. S. Faltas and E. I. Saad, "Slip at the surface of an oscillating spheroidal particle in a micropolar fluid", *ANZIAM J.* **55** (2013) E1–E50.
[29] H. H. Sherief, M. S. Faltas and E. I. Saad, "Slip at the surface of a sphere translating perpendicular to a plane wall in micropolar fluid", *Z. Angew. Math. Phys.* **59** (2008) 293–312; doi:10.1007/s000330076078y.
[30] J. D. Sherwood, "Cell models for suspension viscosity", *Chem. Engrg. Sci.* **61** (2006) 6727–6731; doi:10.1016/j.ces.2006.07.016.
[31] O. M. Sokovnin, N. V. Zagoskina and S. N. Zagoskin, "Choice of boundary conditions for studying the behavior of the swarm of spherical particles traveling through a non-Newtonian liquid", *Theor. Found. Chem. Engrg.* **42** (2008) 366–376; doi:10.1134/S0040579508040040.
[32] J. K. Whitmer and E. Luijten, "Fluid–solid boundary conditions for multiparticle collision dynamics", *J. Phys.: Condens. Matter* **22** (2010) 104–106; doi:10.1134/S0040579508040040.
[33] G. Willmott, "Dynamics of a sphere with inhomogeneous slip boundary conditions in Stokes flow", *Phys. Rev. E* **77** (2008) 055302; doi:10.1103/PhysRevE.77.055302.